NASA Technical Memorandum 106798

Atomic Oxygen Durability Evaluation of the Flexible Batten for the Photovoltaic Array Mast on Space Station

Curtis R. Stidham
NYMA, Inc.
Engineering Services Division
Brook Park, Ohio

Sharon K. Rutledge
National Aeronautics and Space Administration
Lewis Research Center
Cleveland, Ohio

Edward A. Sechkar, David S. Flaherty, and David M. Roig
Cleveland State University
Cleveland, Ohio

Jonathan L. Edwards
Ohio Aerospace Institute
Cleveland, Ohio

Prepared for the
1995 International Solar Energy Conference
cosponsored by ASME, JSME, and JSES
Lahaina, Maui, Hawaii, March 19–24, 1995

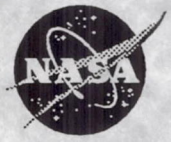

National Aeronautics and
Space Administration

ATOMIC OXYGEN DURABILITY EVALUATION OF THE FLEXIBLE BATTEN FOR THE PHOTOVOLTAIC ARRAY MAST ON SPACE STATION

Curtis R. Stidham
Aerospace Technology Department
NYMA, Inc.
Brook Park, Ohio 44142

Sharon K. Rutledge
Electro-Physics Branch
National Aeronautics and Space Administration
Lewis Research Center
Cleveland, Ohio 44135

Edward A. Sechkar, David S. Flaherty, and David M. Roig
Physics Department
Cleveland State University
Cleveland, Ohio 44115

Jonathan L. Edwards
Ohio Aerospace Institute
Brook Park, Ohio 44142

ABSTRACT

A test program was conducted at the National Aeronautics and Space Administration's Lewis Research Center (LeRC) to evaluate the long term low Earth orbital (LEO) atomic oxygen (AO) durability of a flexible (fiberglass-epoxy composite) batten. The flexible batten is a component used to provide structural rigidity in the photovoltaic array mast on Space Station. The mast is used to support and articulate the photovoltaic array, therefore, the flexible batten must be preloaded for the 15 year lifetime of an array blanket. Development hardware and composite materials were evaluated in ground testing facilities for AO durability and dynamic retraction-deployment cyclic loading representative of expected full life in-space application. The CV1144 silicone (AO protective) coating was determined to provide adequate protection against AO degradation of the composite material and provided fiber containment, thus the structural integrity of the flexible batten was maintained. Both silicone coated and uncoated flexible battens maintained load carrying capabilities. Results of the testing did indicate that the CV1144 silicone protective coating was oxidized by AO reactions to form a brittle glassy (SiO_2) skin that formed cracking patterns on all sides of the coated samples. The cracking was observed in samples that were mechanically stressed as well as samples in non-stressed conditions. The oxidized silicone was observed to randomly spall in small localized areas, on the flexible battens that underwent retraction-deployment cycling. Some darkening of the silicone, attributed to vacuum ultraviolet (VUV) radiation, was observed.

1. INTRODUCTION

Space Station will operate in the low Earth orbital (LEO) environment between the altitudes of 333 to 463 Km and therefore must be designed to withstand the effects of solar radiation, micrometeoroid and space debris impacts, thermal cycling, plasma interactions, and neutral atomic oxygen (AO). Atomic oxygen is the predominant gaseous species in the LEO environment between the altitudes of 180 to 650 Km and is formed by photodissociation of molecular oxygen by solar ultraviolet (UV) radiation[1]. The LEO environment plasma constituents, including atomic oxygen, are present at thermal kinetic energies of approximately 0.1

electron volt (eV). The relative velocity of a spacecraft with respect to the plasma environment (~7.2 Km/s) causes the kinetic energy of the atomic oxygen impacting spacecraft surfaces, normal to ram, to be sufficiently energetic (approximately 4.5 eV) to break many chemical bonds[2]. Organic materials are readily oxidized by AO while some metals form protective oxide layers. Atomic oxygen and UV radiation are cited as the environmental constituents that cause the most damage to the chemistry of polymeric surfaces in LEO[3].

The Space Station photovoltaic array is supported by a Folding Articulated Square Truss Mast (FASTMast) which is used to deploy and retract the solar array blanket (figure 1). The FASTMast is produced by ACE Able Engineering Inc. of Goleta, California. The FASTMast is a repeating truss structure that measures approximately 34.8 meters long and is comprised of 32 bays, each bay measures approximately 77.2 cm on a side by 102.9 cm high[4]. The FASTMast provides the necessary preload on the photovoltaic array blanket when deployed and stores mechanical energy when collapsed into a mast canister upon array stowage into a blanket box. The FASTMast is comprised of structural components that are of metallic construction including longerons, fixed battens and wires, as well as flexible battens that are constructed of fiberglass-epoxy composite. There are four flexible battens per bay. The flexible battens provide the necessary preload to the mast for structural soundness, while still allowing the mast to collapse and be stowed in the mast canister. To achieve the preload necessary for the mast, the flexible battens function in an elastically buckled mode at all times.

The flexible battens, when installed in the FASTMast, are loaded axially at the end pins resulting in bending moments in the bowed battens. The bending moment results in a tensile stress on the outer curved surface fibers and a compressive stress on the inner curved surface fibers. The largest stress value occurs at the center length of the batten and results in a strain of approximately 0.24% when the mast is deployed and 1.5% when retracted. The compressive stress (force/cross sectional area), due to the axial force carried through the batten, is negligible compared to the compressive and tensile stresses resulting from the bending moment.

The flexible battens are made of uniaxial fiberglass-epoxy, approximately 67% S2-glass by volume and 16% resin by weight, and are the most vulnerable to AO degradation of all the FASTMast's structural components. Epoxy has an in-space erosion yield of 1.7×10^{-24} cm^3/atom for AO at a kinetic energy of 4.5 eV[5]. This value is approximately 57% that of polyimide Kapton H, which experiences high rates of oxidation in the LEO environment. The concern is that due to long term (15 year) AO exposure in LEO, the battens will experience a reduction in buckling strength due to the loss of the epoxy resin in the composite and thus a reduction in mast strength.

Previous testing showed that an outer silicone (CV1144) coating exhibited the best AO durability protection and containment of fiberglass[6,7]. These results led to the baseline design of applying a thin silicone (CV1144) coating on the flexible batten to protect the epoxy resin against AO degradation.

This paper presents the results of a test program conducted to verify the performance of the silicone (CV1144) coated flexible batten, under representative loading conditions, to an AO exposure equivalent to a 15 year anti-solar facing AO fluence level on Space Station. The representative loading conditions included static deployment loads during AO durability testing and dynamic loading for retraction-deployment cycling. The battens must be capable of being stowed numerous times during their life on SpaceStation; therefore, the full-length flexible battens were subjected to a total of 35 retraction-deployment cycles during the testing program.

2. APPARATUS AND PROCEDURE

2.1 Materials Evaluated

The batten test samples are a pultruded fiberglass-epoxy with approximately 70% fiberglass (S2-glass) by volume and 16% epoxy resin by weight[8]. All samples had a thin outer coating of epoxy (EA956) and half of the samples had an AO protective silicone (CV1144) coating. The CV1144-0 silicone is a one-part controlled volatility RTV silicone AO protective overcoat produced by McGhan NuSil of Carpenteria, California.

2.1.1 Full-Length Flexible Battens. Four full-length, development hardware, flexible battens (with end fittings) were tested. Samples #1 & #2 were coated with CV1144 silicone while Samples #3 & #4 were uncoated. The dimensions of these four test samples are presented in Table 1. The dimensions were used for determination of the required deflection to produce the targeted level of strain in the battens during AO durability and retracting loading tests. The flexible battens are loaded by axle pins inserted through holes in the end fittings. The pin-pin distance is the distance between the hole centers. The following parameters are the nominal design dimensions for a flexible batten[9]:

Pin-Pin Distance:	80.632 +/- 0.025 cm
Width:	0.953 +0.025/-0.020 cm
Height:	0.699 +0.025/-0.005 cm

2.1.2 Short Batten Samples. Four 15.24 cm batten samples (with no end fittings) were tested. Two samples (C6 & C7) were coated with CV1144 silicone. Two other samples (AO09 & AO10) were uncoated. These samples were used for evaluation of AO undercutting erosion below the protective coating. The samples were exposed to AO under deployed stress conditions.

2.1.3 Mass Witness Samples. Two 3.18 cm long batten segments were used as mass witness samples to gravimetrically determine AO erosion, since mass measurement of the full-length battens or the short (15.24 cm) batten segments was impractical. These two mass witness samples were sectioned from two of the short (15.24 cm) batten samples. One sample (C5) was coated with CV1144 silicone. One sample (AO08) was uncoated. The ends of the mass witness samples were masked with aluminized tape to prevent AO erosion of the unprotected ends. The batten mass witness samples were of the same sample pedigree as the four short (15.24 cm) batten samples.

Polyimide Kapton HN samples (2.54 cm diameter) were used as AO flux dosimeters during AO exposure. All mass witness samples were dehydrated in a vacuum chamber at a pressure between 2.6 and 9.1 Pa (20 to 70 mtorr) prior to mass measurement to eliminate error due to absorbed water and gases. A detailed description on the determination of the dehydration period is presented elsewhere[6].

2.2 Stress Determination

Due to the geometric constraints of the atomic oxygen beam facility, the exposure of the center section of the full-length batten was prohibitive. Therefore, during AO beam exposure, the maximum stress condition at the center of a flexible batten deployed on Space Station was duplicated on the full-length test samples at a point 25.4 cm (10 in) from the end of the batten. This 25.4 cm point was the section of the battens to be evaluated during the testing program. The maximum stress occurring on a flexible batten on Space Station, during retraction, was also duplicated at the 25.4 cm point on the test battens during retraction-deployment cycling.

The stresses were calculated for each individual full-length batten based on its own geometry. The geometry of each batten differed slightly; therefore, the resulting load and strain conditions will differ slightly. The stress conditions for both the AO exposure and the retraction-deployment cycling portions of the test program were calculated based on the pin-pin distances for the on-orbit deployed and stowed conditions - based on development hardware measurements. Development pin-pin distance values of 79.997 cm (31.495 in) for deployed and 57.988 cm (22.830 in) for stowed positions were provided by the Space Station Work-Package IV at LeRC[10]. Stress and strain values were calculated based on the theory of large elastic deflections "Elastica"[11]. A BASIC program was written to solve for the deflection of the batten at any point along its length. The derivation of the formulas used in the program are presented in Appendix A. The short (15.24 cm) batten segments were loaded to the desired stress levels by applying bending moments directly to the ends of the samples. Calculations were performed to obtain the required deflection, at the center of the sample, necessary to provide the desired level of strain. Calculations are presented in Appendix B.

2.2.1 Stress - Atomic Oxygen Exposure. The deployed pin-pin distance for a flexible batten in the FASTMast is 79.997 cm. Using dimensions for Batten #3 and an elastic modulus of 55.2 GPa (8.0×10^6 psi)[9], the resulting maximum compression and tensile stress (due to bending at the batten center) for this pin-pin distance would be 132.4 MPa (19.2 Ksi). This would produce a 0.24% strain. Reproducing this beginning of life (BOL) stress level at the 25.4 cm position results in a pin-pin distance of 79.736 cm (31.392 in). The stress at the center of the batten would now be 158.6 MPa (23.0 Ksi), producing a 0.29% strain for this test pin-pin distance. The predicted load was 230.9 N (51.9 lb). This approach was taken for each of the four battens to determine the pin-pin distance to be maintained during the AO exposure testing (Table 2). The four short (15.24 cm) batten segments were loaded to a strain level of 0.24% by applying bending moments at the ends of the samples, as shown in Appendix B. Nominal dimensions were used to calculate the level of deflection required at a sample's center to provide this level of strain. This deflection value was 0.229 cm (0.090 in), which takes into account the rotation of the mount blocks used to apply the bending moment (according to Appendix B).

2.2.2 Stress - Retraction-Deployment Cycling. The retracted pin-pin distance for the flexible battens in the FASTMast is 57.988 cm (22.830 in). Using dimensions for Batten #3 and an elastic modulus of 55.2 GPa (8.0×10^6 psi)[9] the resulting maximum bending stress at the batten center for this pin-pin distance would be 855 MPa (124 Ksi) with a resulting strain of 1.55%. Reproducing this BOL stress at the 25.4 cm position results in a pin-pin distance of 47.676 cm (18.770 in). The stress at the center is now 154.3 Ksi (1.9% strain) for this new pin-pin distance. The predicted load was 290.6 N (65.3 lb). This approach was taken for each of the four battens to determine the amount of compression required during retraction-deployment cycling (Table 3). This 1.9% strain level is far below the 3.0% strain level warned not to be exceeded by the manufacturer, AEC-Able Engineering Company. The battens were in no danger of breaking at the beginning of the testing program.

2.3 Atomic Oxygen Exposure Process

Atomic oxygen durability testing was performed in the atomic oxygen beam facility at the NASA Lewis Research Center (LeRC). The facility uses a 1000 watt electron-cyclotron resonance (ECR) plasma source, operated on oxygen to generate a low energy, broad area beam consisting of atomic oxygen, ions, radicals, and metastables. The kinetic energy of the directed ionized species has been previously determined, with the use of a retarding potential analyzer probe, to be below 30 electron volts (eV) with a distribution having peaks occurring at 10.5 and 25 eV[12]. The facility vacuum chamber operates at a pressure below 8.0×10^{-2} Pa during ECR source operation. This facility is described in detail in reference 12.

The AO fluence for the durability testing was determined by an effective flux measurement, based on the mass loss of polyimide Kapton HN. Kapton's in-space erosion yield is well known and is an accepted standard of AO flux evaluation[13]. The effective flux measurement, based on dosimeter mass loss, is calculated as follows:

$$Flux_{eff} = \frac{\Delta M}{\rho \times A_s \times t \times EY}$$

ΔM = Change in sample mass (g)
ρ = Density (g/cm^3)
A_s = Sample Area (cm^2)
t = Time (s)
EY = Erosion yield (cm^3/atom)

The in-space erosion yield for Kapton HN is 3×10^{-24} (cm^3/atom), based on an atomic oxygen kinetic energy of 4.5 eV[5,14,15,16,17]. Therefore, the flux calculated gives the equivalent in-space flux required to cause the same mass loss. The error on the flux measurements are typically ±12%[12]. Prior to starting the batten test, a flux map was performed at a distance of approximately 28cm from the end of the plasma source liner, to determine the flux level and distribution of atomic oxygen across the batten exposure position. The distribution was fairly uniform across the mapped region (18 cm diameter), with the effective flux ranging from 3×10^{16} to 4×10^{16} (atoms/cm^2·s). Based upon this flux map, the effective flux was calculated for each batten position based on the mass loss of Kapton dosimeters. The effective fluence is determined by simply multiplying the effective flux for each location by the exposure duration.

The flexible battens in the FASTMast will be exposed to different AO flux levels in LEO, depending on their location within the mast. To take a conservative approach in the testing procedure, the test battens were exposed to the maximum 15 year anti-solar facing fluence level of 5.4×10^{22} (atoms/cm^2). The full-length flexible battens and the short (15.24 cm) batten segments were under deployed load conditions during AO exposure. The full-length battens were mounted in the batten mount frame which was designed to maintain a fixed pin-pin distance on all four full-length battens (figure 2). The photograph (figure 2) shows the battens before AO exposure. The battens were exposed with one side normal to the atomic oxygen arrival, thus providing exposure to both the tensile and compressed fibers on the same surface. This provided repetitive surfaces for evaluation and an even flux distribution across the battens. During exposure, the tensile and compressive surfaces received atomic oxygen exposure. The load present during AO exposure was monitored on (full-length) Battens #2 & #3 using load cells located in the Batten Mounting Frame. The loads, sampled every 30 seconds, were compiled with a computer. The battens were loaded to the predetermined pin-pin distance for each AO exposure period. Following each AO exposure period, the battens were maintained at their deployed load conditions in the batten mount frame until they were removed just prior to undergoing retraction-deployment cycling. Following retraction-deployment cycling, the battens were photographed (24X) at the 25.4 cm position and at the batten center.

The short (15.24 cm) batten sections were also exposed with one side normal to the AO arrival. The center point of these batten sections were centered under the beam with the BOL bending strain level of approximately 0.24% throughout the length of the sample. A mounting fixture was designed to apply bending moments at both ends of the samples to produce this strain. The deflection at the center of the section was measured with a linear variable differential transformer (LVDT) to determine when the appropriate BOL strain level was achieved. This mounting fixture was then attached to the batten mount frame (figure 2). In this photograph, the two batten mass witness samples and the AO flux dosimeter can be seen. The 2.54 cm diameter dosimeters are Kapton HN, mounted inside aluminum foil to prevent erosion from the side. The other 2.54 cm diameter samples were CV1147 coated Kapton and SiO_x coated Kapton present for another experiment.

Two free standing thermocouples (no surface contact) were used during AO exposure Series #3, which was the longest single exposure period, to estimate the temperature of the battens during testing. The thermocouples had an exposed junction covered with Kapton tape. This technique is typically implemented in AO durability testing when contact can not be made with critical surfaces.

2.4 Retraction-Deployment Cycling

An Instron Series IX Automated Materials Testing System (1.09) was used for the retraction-deployment cycling tests (figure 3). The load and the head displacement (stroke)

were measured during the compression stroke. The compression rate was 0.635 (cm/s) and the data was sampled at a rate of 10 Hz. The four full-length flexible battens each underwent 35 cycles during the testing program. This number was provided by LeRC Space Station Work-Package IV to represent a conservative number of retraction cycles expected during the lifetime of a photovoltaic array blanket[18]. During the retraction cycle, the battens were compressed a distance of approximately 32.94 cm (12.97 in). This retraction is 10.31 cm (4.06 in) greater than what a flexible batten will experience in the FASTMast. This distance was determined to produce the same stress, at the off center (25.4 cm from end) position of the test samples, as a batten in the FASTMast will experience at its center point when stowed in the Mast Canister. Since the system utilized a single control program, the compression distance for each flexible batten was the same. The 32.94 cm nominal retraction that was used represents the average retraction distance calculated for the four full-length flexible batten samples. All five series of retraction cycle tests were video taped to provide a record of the test and to capture any potential failures of the battens, were they to occur. At the beginning of the testing program, the battens were in no danger of breaking, since the maximum strain at the center of each flexible batten was below the 3.0% strain limit set by the manufacturer.

3. RESULTS & DISCUSSION

3.1 Atomic Oxygen Durability Results

The battens were exposed to AO during five separate exposure periods, for a total of 447 hours. The total Kapton effective fluence for the full-length flexible battens ranged from 5.30×10^{22} to 5.75×10^{22} (atoms/cm^2), thus less than an 8% variation existed in the fluence across the test points on the full-length flexible battens. This variation in fluence is attributed to the battens' exposure positions in the beam. Based on a 15 year (anti-solar facing) fluence of 5.4×10^{22} (atoms/cm^2), the equivalent in-space lifetimes for the full-length flexible battens ranged from 14.7 to 16.0 years. The total Kapton effective fluence for the short (15.24 cm) batten segments ranged from 5.25×10^{22} to 5.77×10^{22} (atoms/cm^2), thus a 9% variation existed in the fluence across the test points on these samples. The batten mass witness samples C5 and AO08 experienced a total effective fluence of 4.52×10^{22} and 4.54×10^{22} (atoms/cm^2) respectively. The effective fluence levels for each sample is presented in Table 4. The maximum temperature measured during AO exposure Series #3 was 86 Celsius.

The 3.18 cm long batten mass witness samples were used to determine the mass loss per unit area of the batten materials as a function of AO fluence. The results are presented in figure 4. The uncoated sample experienced a total mass loss that was greater than five times that of the silicone coated sample. As can be seen in the plot, the uncoated sample seemed to undergo the majority of its mass change (≈70%) after the first exposure series. This is attributed to the loss of the outer epoxy layer that is applied to the battens. The full-length uncoated battens experienced what appeared to be total removal of the outer epoxy layer in the region of the 25.4 cm position along the batten (position located directly under the beam). By the end of the AO exposure tests, visual inspection revealed that the uncoated full-length flexible battens and the short (15.24 cm) batten segments had undergone complete removal of the outer epoxy layer. Even the areas not under direct AO exposure lost the outer epoxy layer due to attack by the background oxygen plasma. The loss of the outer epoxy layer is evident in the photographs taken of the battens following the last AO exposure (figure 5) where the white appearing battens are those that were not coated with silicone.

The mass loss per unit area as a function of fluence curve (figure 4) for the CV1144 coated batten has a similar shape to that for the uncoated batten; however, the magnitude of the material loss is much less. At an AO effective fluence level of 4.5×10^{22} (atoms/cm^2), equivalent to 12.5 years on Space Station, the coated and uncoated samples experienced a per unit area mass loss of 0.568 and 2.998 mg/cm^2 respectively. The initial mass loss rate for the coated batten is probably due to a combination of epoxy loss at the sites where the CV1144 coating did not completely cover the batten and loss of organic groups from the silicone. As the CV1144 oxidizes it should pick up oxygen to form SiO_2 at the surface and may gain a small amount of weight. As the epoxy oxidizes, glass fibers will be exposed and the reaction should slow down due to the reduced epoxy exposure area. It appears that the epoxy loss is the dominant reaction here, because the batten continues to lose mass rather than gain and the knee in the curve occurs at the same place as the uncoated batten. This indicates that the slowing of material loss for the coated material may be due to the increased area of fiberglass exposed, similar to the uncoated batten. Small defects in the CV1144 coating were visibly (24X magnification) evident at the beginning of the testing program. Defects included scratches and particulates under the coating. The defects became more evident as AO exposure progressed. This can be seen in photograph (figure 6) of Batten #1 after the second AO exposure; (a small section of silicone was missing which exposed the underlying fibers).

The silicone oxidizes in the AO environment to form a glassy brittle surface. Cracking of this glassy surface was observed on all four sides of (full-length) Battens #1 & #2. The cracks on the tensile side were perpendicular to the fiber direction and parallel to each other (figure 7). The cracks on the remaining three sides were non-uniform in

direction (figure 8) and had a webbed appearance, (similar to that of dried mud). These three surfaces were under some degree of compressive stress. This non-uniform cracking was more pronounced on the compression side and exposed (ram) side than on the anti-ram side. The formation of cracking was evident following the first series of AO exposure followed by the second series of retraction-deployment cycling. The cracking became more severe with increased testing. These same cracking results were observed on the short (15.24 cm) batten segments (C6 & C7). The coated mass witness sample (C5), which was not stressed during testing, experienced the non-uniform directional cracking pattern on its three exposed surfaces, with the most pronounced cracking evident on the ram (normal to beam) surface.

The uncoated battens appeared to have nearly all of the outer epoxy removed, resulting in exposure of the fiberglass (figure 9) which fractured upon retraction-deployment cycling of the full-length samples. Large amounts of frayed exposed fibers were not observed, as was seen previously in long duration radio frequency (13.56 MHz) air plasma asher tests of longerons[6,7], but some fibers did become separated and free standing (figure 10). The extent of AO erosion observed on the uncoated full-length battens could result in the formation of a source for particulate contamination, within the 15 year lifetime of Space Station. The arrival of AO in this test was basically unidirectional, therefore the fiberglass provided shielding to the underlying epoxy. In previously conducted plasma asher tests[6,7], AO arrival was random and the epoxy was more vulnerable below the fiberglass. The silicone coated battens did not experience fiber separation.

There was visible evidence of UV darkening of the silicone coated test samples at the end of AO testing. Figure 11 shows the silicone coated mass witness sample (C5) next to a pristine segment of the same sample material. Darkening of the uncoated batten samples was not observed. Figure 12 shows the uncoated mass witness sample (AO08) next to a pristine segment of the same sample material. Therefore, the darkening is not suspect of contamination produced in the test facility. In the atomic oxygen beam facility, the ECR plasma source produces intense vacuum ultraviolet (VUV) radiation as occurs in radio frequency (RF) plasma ashers[19], particularly at the 130 nm characteristic resonance line for oxygen. Evidence of VUV radiation produced in the ECR plasma was the discoloration of zinc orthotitanate/potassium silicate thermal control coatings previously tested, which also occurs when exposed to an RF plasma asher[20]. Tests conducted after this testing program was completed, confirmed the presence of intense VUV radiation produced by the ECR plasma source. A photomultiplier tube (PMT) coated with sodium salicylate was used with a bandpass filter and a MgF_2 window to obtain the VUV content of the ECR source from 125 to 180 nm[21]. The intensity within this wavelength range was determined to be approximately 150 VUV equivalent suns. The total radiation exposure, resulting from the 447 hours of AO exposure, resulted in an excess of 67×10^3 VUV equivalent sun hours. This represents approximately 80% to 84% of the full life VUV radiation exposure for solar facing surfaces on the Space Station photovoltaic array[22].

The short (15.24 cm) batten segments were cut into sections so that erosion depth could be investigated. The batten segments were cut with a silicon-carbide abrasive saw, which was somewhat damaging to the surfaces of the samples, thus making a definitive evaluation as to the depth of undercutting difficult. The silicone coating on batten segments (C6 & C7) appeared to remain intact. Even with the cutting procedure, there was no obvious points of AO erosion or damage from cutting beyond the fourth or fifth fiber layer. A scanning electron beam micrograph of sample C6 (figure 13) shows this. The uncoated batten segments (AO09 & AO10), did have free fibers exposed at the surface upon completion of AO durability testing. The cutting process appeared to be more destructive, since when the fibers were severed, they were pulled by the abrasive wheel. Based on fiber separation from the bulk composite, the ability of the epoxy being unable to hold fibers within the composite, was to a depth of approximately 10 fiber layers from the surface. This is shown in the optical micrograph (figure 14) of sample AO09, shown mounted in a metallurgy mounting compound.

Load cells were used to monitor the loads in-situ on (full-length) Battens #2 & #3 during all five AO exposure series. Dramatic changes were observed in the load on Batten #2 during the last three AO exposures and on Batten #3 during all of the AO exposure series. These changes were later revealed to be a result of the load cells' responses to environmental changes and was not attributable to load changes in the battens. Following the last series of AO exposures, the load cells were tested unloaded and with no means of developing a load (no battens present), to see their response to environmental changes. The same magnitude of changes were observed. The load cells were recalibrated following the testing program and were found to have had no change in calibration; therefore, the load cells provided reliable load values at atmospheric pressure (initial loads on the battens were known). The initial deployed loads on Battens #2 & #3 are shown in figure 15 for each of the five AO exposure series. As can be seen from the plot, the initial loads were nearly constant for all five series, with the slight differences attributable to the measurement uncertainty in the actual pin-pin distance of the battens in the Batten Mounting Frame. Since the magnitude of the load changes observed during AO exposure of the battens matched those observed by the load cells alone, the battens did not experience a notable change

cells alone, the battens did not experience a notable change in load during AO exposure.

3.2 Retraction-Deployment Cycling Results

The four full-length flexible battens each underwent 35 retraction-deployment cycles during the testing program. Each batten was compressed to a nominal distance of 32.94 at the rate of 0.635 cm/s. A summary of the retraction-deployment series and their occurrence in relation to AO exposure testing is presented in Table 5.

Typical load versus displacement (compression) plots for the four full-length battens are shown in figures 16-19. These plots show the results from the first retraction cycle for each batten in the Instron and the theoretical curve determined from the theory of "Elastica". As can be seen, there is a slight difference in the predicted values and the experimentally determined curves. The calculations assumed the fiberglass-epoxy composite material was isotropic in nature. The error in the load calculated for the desired stress conditions was low (<6.4%) for the deployed load level, compared to the results from the first retraction cycle in the Instron Instrument (figures 16-19). This error may be attributed to the fact that the battens had a very slight initial curvature which is not accounted for in the calculated values. The battens were assumed to be ideally straight. Also, the dimensions of the battens were not accurately known due to the uncertainty in the thickness of the outer epoxy and silicone coatings. Therefore, the predicted values were in close agreement with the experimental results.

The load values at only two distinct compression points (32.77 cm and 22.63 cm) were plotted versus the retraction cycle (see figures 20-23). The 32.77 cm is the amount of retraction for the test and the 22.63 cm corresponds to the retraction distance of the flexible batten in the FASTMast. From these plots we see an interesting result. As the battens are cycled during a single series, each consecutive load is typically less than the previous; however, following an AO exposure, the next series of retraction cycles starts at a higher load level than the ending of the previous retraction series. The reason for this phenomenon is unknown. In the plots, the dashed line provides a first order estimate of the trend in the load change. Finally, the retraction load at the 32.77 cm compression distance was plotted verses AO effective fluence(figure 24). The phenomenon just mentioned is much more evident from this plot's sawtooth pattern, where there is an increase in load following an AO exposure. The overall range in loads between all the battens was 15.9 N, but for an individual batten, the largest load variation was 6.4 N (Table 6). The greatest variation in loads occurred for Battens #1 & #2 which are silicone coated, and the greater required load for retraction, though minimal, was demonstrated by the uncoated Battens #3 & #4.

During the first cycle of a retraction loading series, a distinct "ping" type sound could occasionally be heard during the retraction, perhaps due to the snapping of a glass fiber or fibers. This only occurred for the first cycle in a retraction series that followed AO exposure. The sound could be heard from one to a few times during the first cycle, but was not heard during the remainder of the cycles for that series. This sound was evident for Battens #3 & #4. Finally, no fractures to the bulk material occurred in any of the full-length flexible battens during the tests.

4. CONCLUSIONS

The CV1144 silicone protective coating was demonstrated to provide sufficient AO protection for the fiberglass-epoxy composite materials used for the flexible batten. The CV1144 silicone coated sample observed a per unit area mass loss that was less than 19% that experienced by the unprotected material. The uncoated batten samples experienced complete removal of the outer epoxy layer exposing fiberglass that fractured upon retraction-deployment cycling. The AO erosion of an uncoated batten could result in the formation of a source for particulate contamination within the 15 year lifetime of Space Station. The silicone coated battens developed a brittle glassy coating on the surface of the silicone that became fractured, even in the unstressed condition, but in general remained adherent and continued to provide AO protection and containment of the fiberglass. Both the silicone coated and uncoated full-length flexible battens maintained load carrying capabilities with the greatest variation in buckling load being 2.3% at a compression distance of 32.77 cm over the simulated 15 year lifetime of Space Station.

5. ACKNOWLEDGMENTS

The authors wish to gratefully acknowledge Demetrios Papadopoulos, Case Western Reserve University, and Charles Pennington, NASA Lewis Research Center, for their significant contributions in conducting deployment-retraction cyclic testing.

6. REFERENCES

1. NOAA, NASA, and USAF, U.S. Standard Atmosphere, 1976, NASA TMX-74335, 1976, pp. 12-15.

2. J.T. Visentine and L.J. Leger, "Material Interactions With the Low Earth Orbital Environment: Accurate Reaction Rate Measurements," JPL Publication 87-14, pp. 11-20, November 1986.

3. J.A. Dever, "Low Earth Orbital Atomic Oxygen and Ultraviolet Radiation Effects on Polymers," NASA Technical Memorandum 103711, February 1991.

4. Lockheed Missiles & Space Company, Inc., Space Station Freedom WP-4, Solar Array Photovoltaic Win g, Critical Design Review, Vol. 1, Section 5.5, 1-2 December, 1992.

5. L.G. Leger, B. Santos-Mason, J.T. Visentine, and J.F. Kuminecz, "Review of LEO Flight Experiments," in Proceedings of the NASA Workshop on Atomic Oxygen Effects, D.E. Brinza, ed., NASA CR-181163 (NASA Washington, D.C., 1987) pp. 1-10, November 1986.

6. S.K. Rutledge, P.E. Paulsen, J.A. Brady, and M.L. Ciancone, "Oxidation and Protection of Fiberglass-Epoxy Composite Masts for Photovoltaic Arrays in the Low Earth Orbital Environment," NASA Technical Memorandum 100839, April 1988.

7. S.K. Rutledge, P.E. Paulsen, and J.A. Brady, "Evaluation of Atomic Oxygen Resistant Protective Coatings for Fiberglass-Epoxy Composites in LEO," NASA Technical Memorandum 101955, May 1989.

8. D. Ma, personal communications, Lockheed Missiles & Space Company, Inc., 22 July, 1992.

9. P. E. Paulsen, personal communications, National Aeronautics and Space Administration (Space Station Program WP-4), 23 October, 1992.

10. W. Barlett, personal communications, National Aeronautics and Space Administration (Space Station Program WP-4), 13 December, 1992.

11. S.P. Timshenko and J.M. Gere, Theory of Elastic Stability, McGraw-Hill Book Company, Inc., New York, New York, 1961, pp. 76-82.12.

12 C.R. Stidham, et.al., "Low Earth Orbital Atomic Oxygen Environmental Simulation Facility for Space Materials Evaluation," in Bailey, V. et. al., eds., Proceedings of the 38th International SAMPE Symposium and Exhibition, Advanced Materials: Performance Through Technology Insertion, Science of Advanced Materials and Process engineering Series, Volume 38, Book 1, 1993, Society for the Advancement of Materials and Process Engineering, Covina, CA., 1993, pp. 649-663.

13. B. Banks, et.al., "Atomic Oxygen Durability Evaluation of Protected Polymers Using Thermal Energy Plasma Systems," Paper for presentation at the International Conference of Plasma Synthesis and Processing of Materials, Denver, Colorado, 21-25 February 1993.

14. L.G. Leger, "Oxygen Atom Reaction With Shuttle Materials at Orbital Altitudes - Data and Experiment Status," AIAA Paper 83-0073, January 1983.

15. L.G. Leger, I.K. Spiker, J.F. Kuminecz, T.J. Ballentine, and J.T. Visentine, "STS Flight 5 LEO Effects Experiment -- Background Description and Thin Film Results," AIAA Paper 83-2361-CP, November 1983.

16. J.T. Visentine, L.G. Leger, J.F. Kuminecz, and I.K. Spiker, "STS-8 Atomic Oxygen Effects Experiment," AIAA Paper 85-0415, January 1985.

17. D.R. Coulter, R.H. Liang, S.H. Chung, K.O. Smith, and A. Gupta, "O-Atom Degradation Mechanisms of Materials," in Proceedings of the NASA Workshop on Atomic Oxygen Effects, D.E. Brinza, ed., NASA CR-181163 (NASA Washington, D.C., 1987) pp. 1-10, November 1986.

18. M. Felder, personal communications, National Aeronautics and Space Administration (Space Station Program WP-4), December, 1992.

19. S.L. Koontz, K. Albyn, and L.J. Leger, Journal of Spacecraft and Rockets, 28,(3), 315, (1991).

20. J.A. Dever and E.J. Bruckner, "The Effects of RF Plasma Ashing on Zinc Orthotitanate/Potassium Silicate Thermal Control Coatings," AIAA Paper No. 92-2171-CP, April 1992.

21. J.A. Dever, personal communications, National Aeronautics and Space Administration, 15 August, 1994.

22. J. Brady and B. Banks, "Vacuum Ultraviolet Radiation and Thermal Cycling Effects on Atomic Oxygen Protective Photovoltaic Array Blanket Materials," in Materials Degradation in Low Earth Orbit (LEO), V. Srinivasan and B.A. Banks, eds., The Minerals, Metals and Materials Society, 1990, pp. 133-143.

TABLE 1: FULL-LENGTH SAMPLE DIMENSIONS

Sample No.	CV1144 Coated	Pin-Pin Distance(cm)	Width (cm)	Height (cm)
1	Yes	80.615	0.962*	0.715*
2	Yes	80.622	0.962*	0.715*
3	No	80.602	0.963	0.719
4	No	80.627	0.960	0.711

*Average width/height dimensions from Batten #3 & #4 were used in the calculations to determine the required deflection to produce the targeted levels of strain for Batten #1 & #2 since the silicone protective coating does not contribute to the battens' flexural rigidity.

TABLE 2: AO EXPOSURE BATTEN CONDITIONS

Sample #	Pin-Pin Distance (cm)	Load (N)	Strain (%) @ 25.4 cm Position	Strain (%) @ Center Position	Compression Distance (cm)
1	79.731	228.2	0.24	0.29	0.884
2	79.728	228.2	0.25	0.29	0.894
3	79.736	230.9	0.24	0.29	0.866
4	79.723	222.9	0.24	0.29	0.904

TABLE 3: BATTEN CONDITIONS FOR RETRACTION LOADING

Sample #	Pin-Pin Distance (cm)	Load (N)	Strain (%) @ 25.4 cm Position	Strain (%) @ Center Position	Compression Distance (cm)
1	47.676	287.4	1.55	1.93	32.939
2	47.663	287.4	1.55	1.93	32.959
3	47.676	290.5	1.55	1.93	32.926
4	47.655	280.2	1.54	1.91	32.972

TABLE 4: TOTAL ATOMIC OXYGEN EXPOSURE

Sample No.	Effective Fluence (Atoms/cm^2) x 10^{22}	Equivalent* Years In-Space
1	5.50	15.2
2	5.75	16.0
3	5.61	15.6
4	5.30	14.7
AO10	5.25	14.6
AO09	5.77	16.0
C7	5.75	16.0
C6	5.47	15.2
AO08	4.54	12.6
C5	4.52	12.6

*Equivalent years in-space are based on an annual atomic oxygen fluence of 3.6×10^{21} atoms/cm^2.

TABLE 5: RETRACTION CYCLING OCCURRENCE

Retraction Series	Number of Cycles	Retraction Series Followed AO Exposure Series
1	4	Before AO
2	4	1
3	9	2
4	9	3
5	9	5

TABLE 6: RETRACTION LOAD RANGE

Sample No.	Minimum Load (N) at 32.77 cm	Maximum Load (N) at 32.77 cm	Load Range (N)	Variation in Load (%)
1	268.5	274.9	6.4	2.3
2	272.0	276.6	4.6	1.7
3	280.9	284.4	3.5	1.2
4	276.7	279.9	3.2	1.1

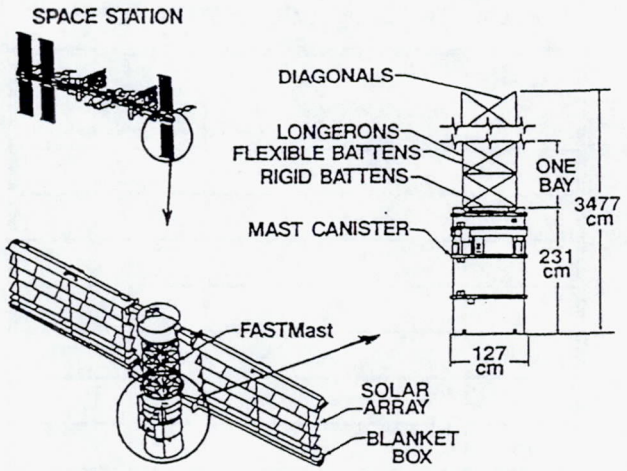

FIGURE 1: SCHEMATIC OF FASTMast

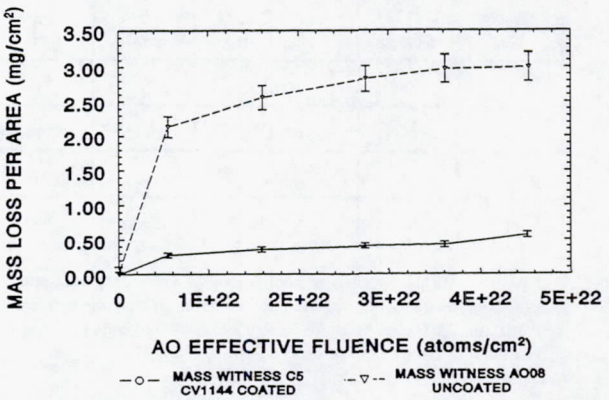

FIGURE 4: BATTEN MASS LOSS PER UNIT AREA AS A FUNCTION OF AO FLUENCE

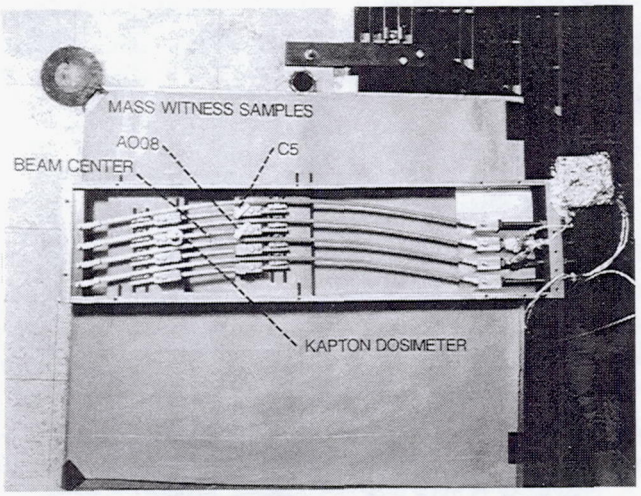

FIGURE 2: TEST SAMPLES BEFORE AO EXPOSURE

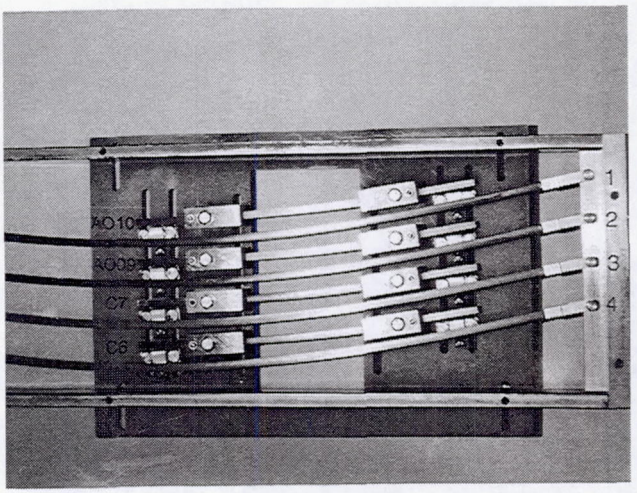

FIGURE 5: TEST SAMPLES FOLLOWING AO EXPOSURE

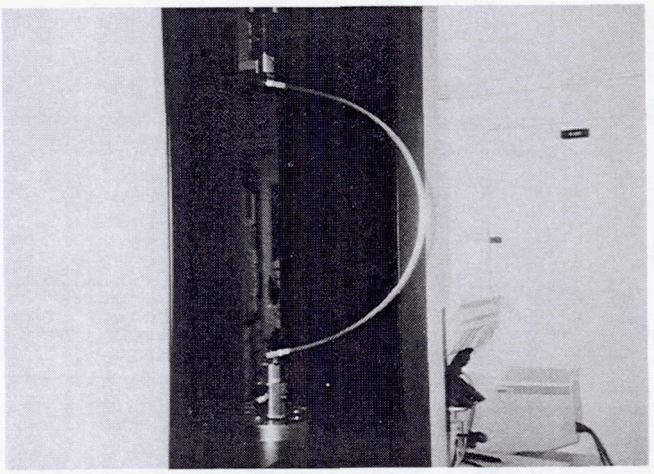

FIGURE 3: FLEXIBLE BATTEN RETRACTION-DEPLOYMENT CYCLING

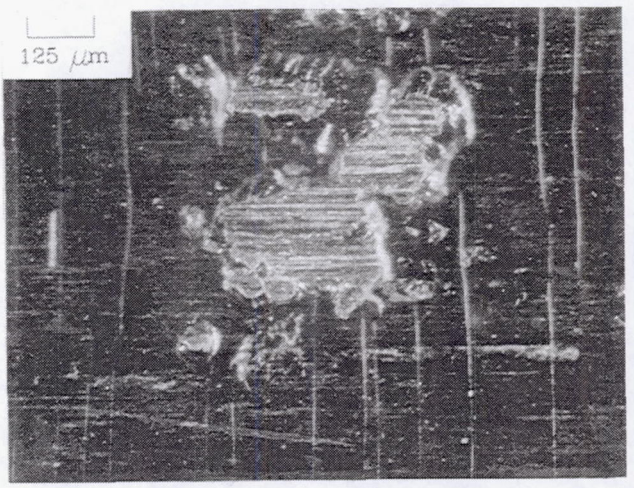

FIGURE 6: SAMPLE #1 AT 25.4 CM POSITION (TENSILE SIDE) FOLLOWING SECOND AO EXPOSURE

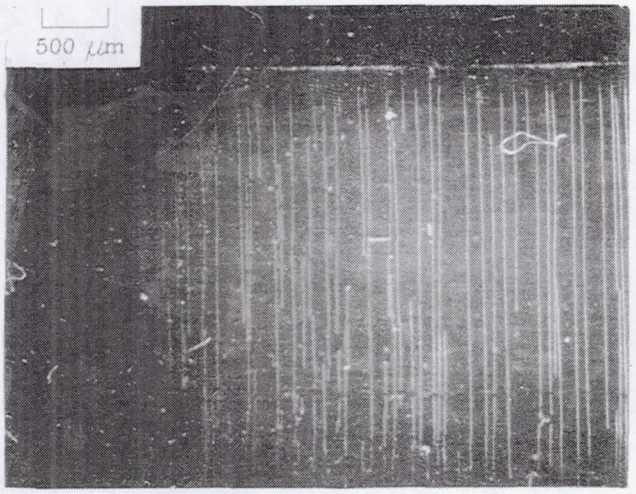

FIGURE 7: SAMPLE #1 PARALLEL CRACKING PATTERN ON TENSILE SIDE

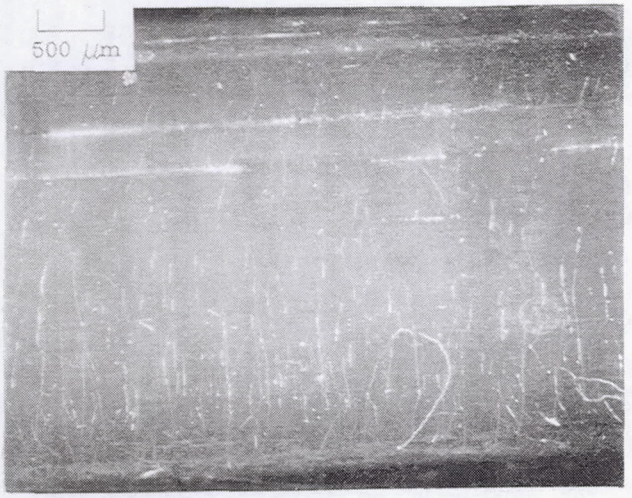

FIGURE 8: SAMPLE #1 NON-DIRECTIONAL CRACKING PATTERN ON RAM SIDE

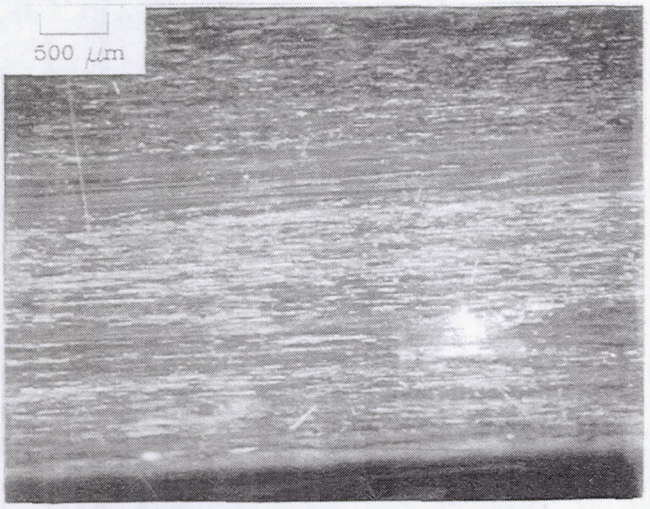

FIGURE 9: SAMPLE #4 EROSION OF OUTER EPOXY LAYER

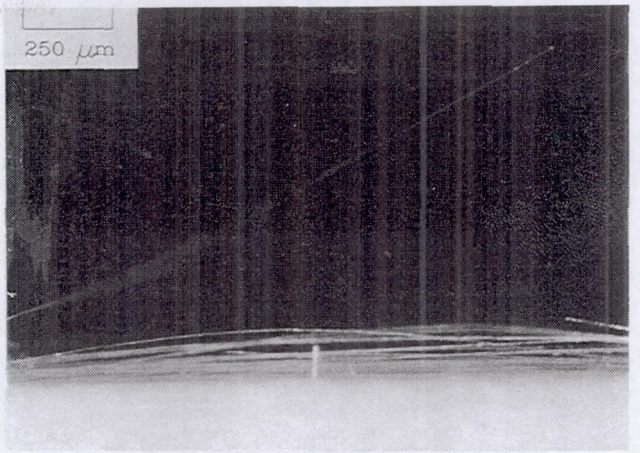

FIGURE 10: SAMPLE #4, FIBERGLASS SEPARATION FROM COMPOSITE

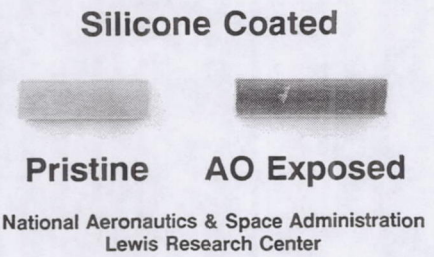

FIGURE 11: EXPOSED AND PRISTINE CV1144 COATED BATTEN MATERIAL

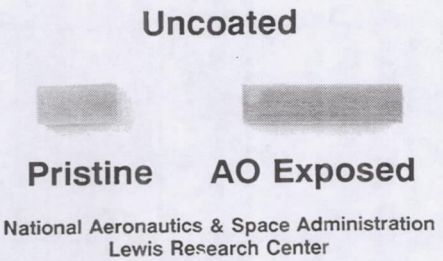

FIGURE 12: EXPOSED AND PRISTINE UNCOATED BATTEN MATERIAL

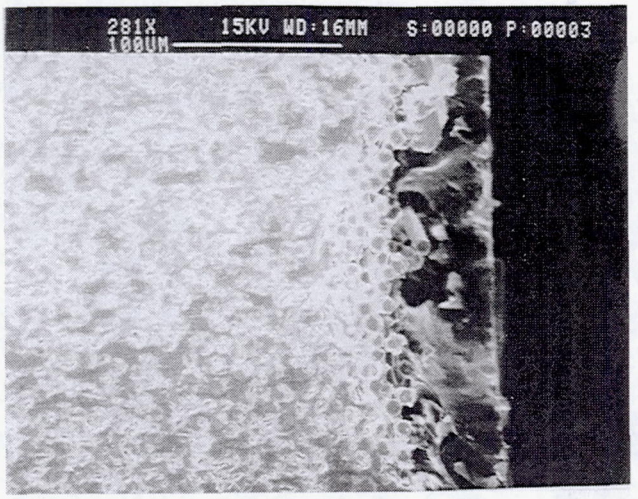

FIGURE 13: SEM MICROGRAPH OF CROSS SECTIONED SAMPLE C6

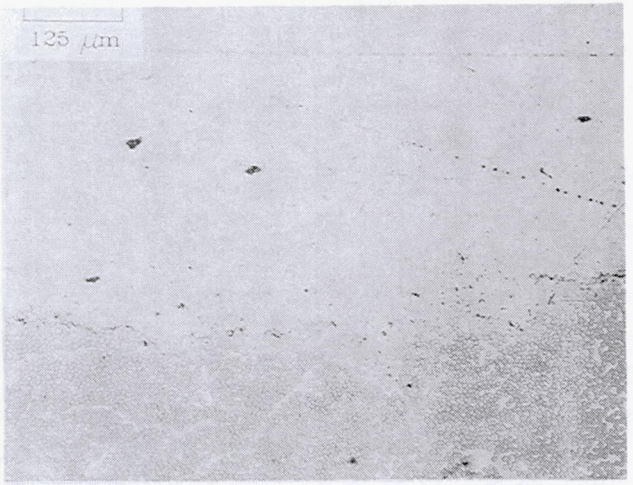

FIGURE 14: MICROGRAPH OF CROSS SECTIONED SAMPLE AO09

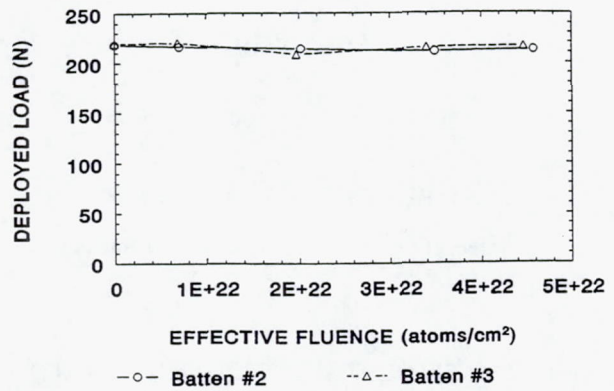

FIGURE 15: DEPLOYMENT LOADS ON SAMPLES #2 & #3 DURING AO EXPOSURE TESTING

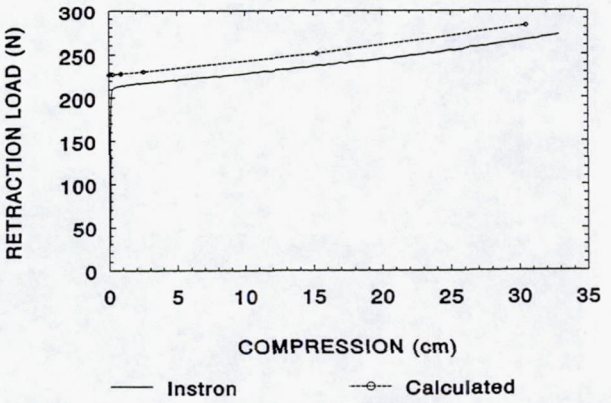

FIGURE 16: SAMPLE #1 LOADS AS A FUNCTION OF COMPRESSION DISTANCE

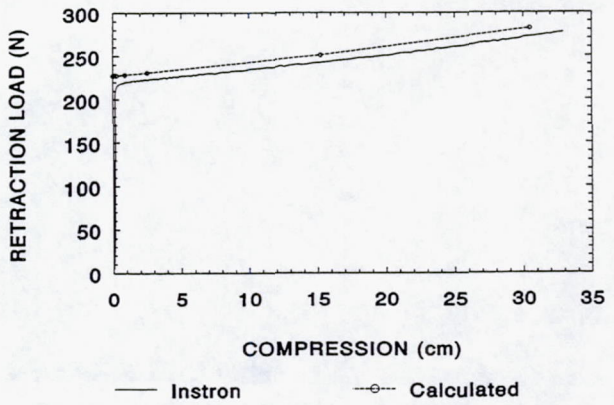

FIGURE 17: SAMPLE #2 LOADS AS A FUNCTION OF COMPRESSION DISTANCE

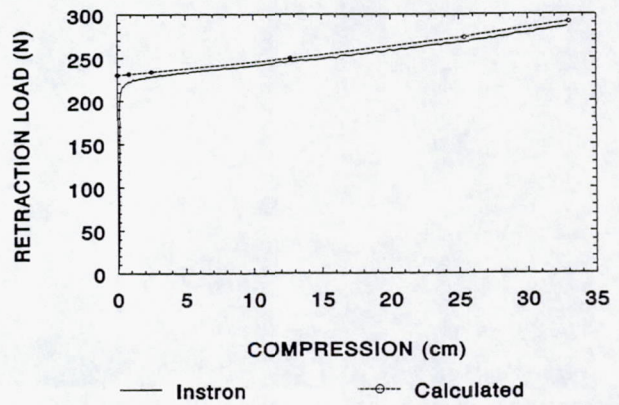

FIGURE 18: SAMPLE #3 LOADS AS A FUNCTION OF COMPRESSION DISTANCE

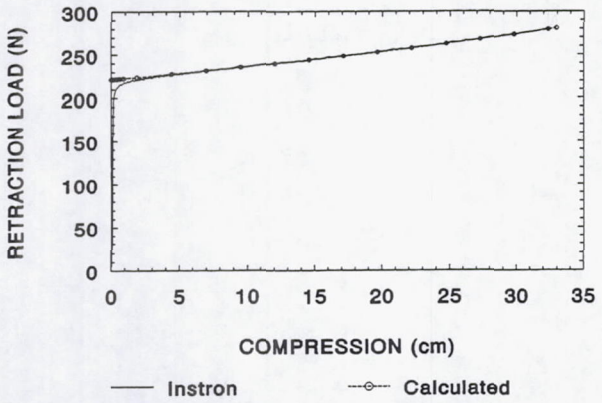

FIGURE 19: SAMPLE #4 LOADS AS A FUNCTION OF COMPRESSION DISTANCE

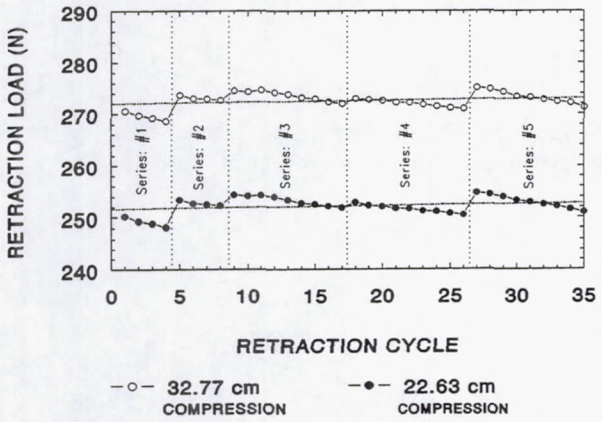

FIGURE 20: SAMPLE #1 RETRACTION LOAD AS A FUNCTION OF RETRACTION CYCLE

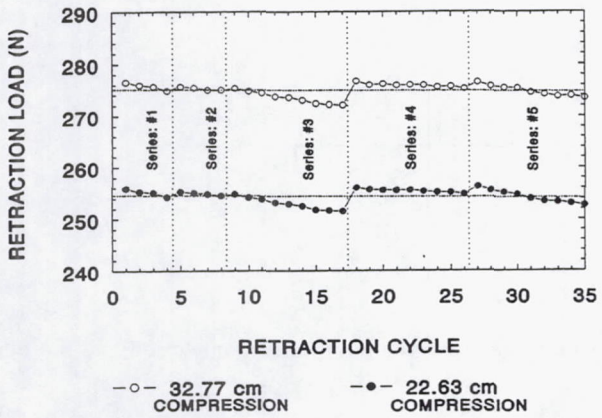

FIGURE 21: SAMPLE #2 RETRACTION LOAD AS A FUNCTION OF RETRACTION CYCLE

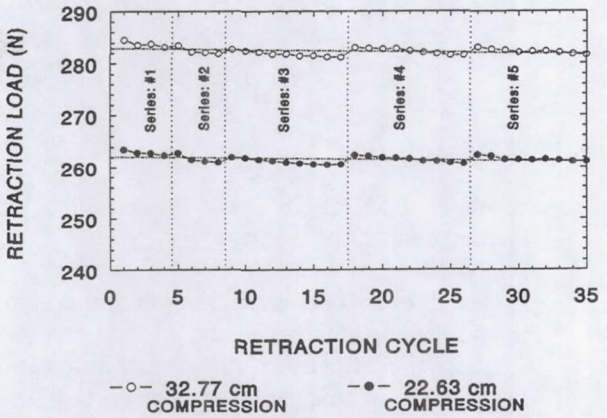

FIGURE 22: SAMPLE #3 RETRACTION LOAD AS A FUNCTION OF RETRACTION CYCLE

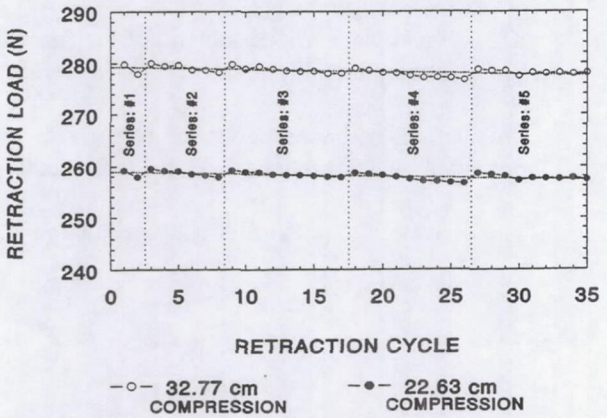

FIGURE 23: SAMPLE #4 RETRACTION LOAD AS A FUNCTION OF RETRACTION CYCLE

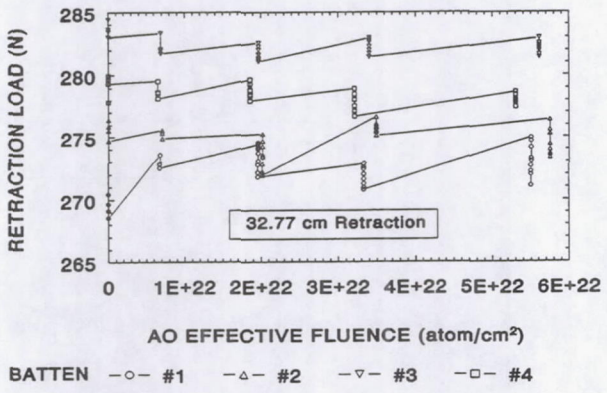

FIGURE 24: RETRACTION LOAD AS A FUNCTION OF AO EFFECTIVE FLUENCE

APPENDIX A

Derivation of Full Length Flexible Batten Deflection

Symbols

E: elastic modulus, Pa
I: area moment of inertia, m^4
P: axial load, N
L: length of half the batten pin-pin distance, m
S: arc length along batten, m
y: deflection of batten perpendicular to force direction, m
x: position for calculation of y for given β, m
k: defined constant, m^{-1}
C: constant of integration, m^{-2}
Θ: angle between tangent to arc and horizontal, °
α: angle between tangent to arc and horizontal at x=0, °
β: angle between tangent to arc and horizontal at (x,y), °
ϕ: defined angle, °
ρ: defined constant $\sin(\alpha/2)$
$K(\rho)$: complete elliptic integral of the first kind
$E(\rho)$: complete elliptic integral of the second kind

Calculations of batten deflection at a given position along the length of the batten are derived from the theory presented by Timoshenko & Gere (reference 11) for large elastic deflections at the center of a rod.

The derivation uses the following geometry:

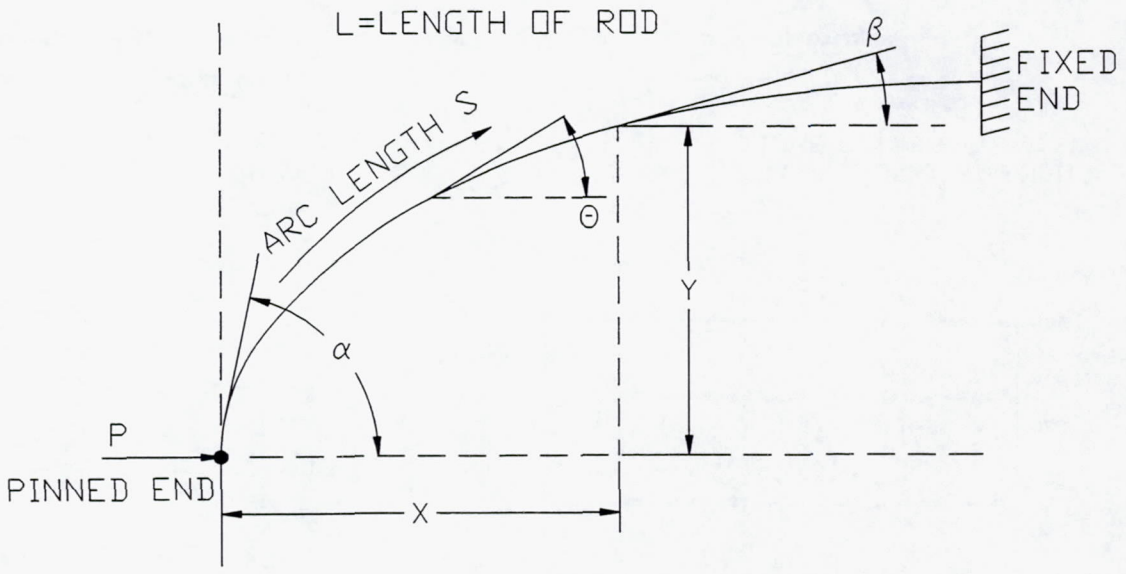

This represents one half of the batten loaded at both ends, with one end having a pinned connection and the other being fixed.

If Θ is the angle between the tangent and the horizontal, then the curvature is;

$$\frac{ds}{d\theta}$$

The bending moment of the bar is equal to the flexural rigidity times the curvature, i.e.

$$E\ I\ \frac{d\theta}{ds} = -P\ y$$

$$\frac{dy}{ds} = \sin\theta$$

Using the above and differentiating with respect to s, yields;

$$E\ I\ \frac{d^2\theta}{ds^2} = -P\ \sin\theta$$

To begin solving this equation, make the following substitution;

$$k^2 = \frac{P}{E\ I}$$

multiply both sides by $d\Theta$, and integrate;

$$\int \frac{d^2\theta}{ds^2}\ \frac{d\theta}{ds}\ ds = -k^2 \int \sin\theta\ d\theta$$

This equation can also be expressed as;

$$\frac{1}{2} \int \frac{d}{ds}\ \left(\frac{d\theta}{ds}\right)^2 ds = -k^2 \int \sin\theta\ d\theta$$

and when integrated becomes;

$$\frac{1}{2}\left(\frac{d\theta}{ds}\right)^2 = k^2\ \cos\theta + C$$

where C is determined form the boundary conditions of the batten.

At the top of the batten;

$$\frac{d\theta}{ds} = 0, \quad \theta = \alpha$$

which gives;

$$C = -k^2\ \cos\alpha$$

Substituting this result gives;

$$\left(\frac{d\theta}{ds}\right)^2 = 2k^2\,(\cos\theta - \cos\alpha)$$

or;

$$\frac{d\theta}{ds} = \pm\, k\sqrt{2}\sqrt{\cos\theta - \cos\alpha}$$

Dropping the positive sign, since dΘ/ds is always negative, and solving for ds gives;

$$ds = -\frac{d\theta}{k\sqrt{2}\sqrt{\cos\theta - \cos\alpha}}$$

or by using various trigonometric identities gives;

$$ds = -\frac{1}{2\,k}\frac{d\theta}{\sqrt{\sin^2\frac{\alpha}{2} - \sin^2\frac{\theta}{2}}}$$

The arc length between any two values of Θ is found by integrating over the appropriate interval. As s increases from 0 to L, Θ decreases from α to 0. The value of L is known,

$$L = \int ds = \int_{\alpha}^{0} -\frac{1}{2\,k}\frac{d\theta}{\sqrt{\sin^2\frac{\alpha}{2} - \sin^2\frac{\theta}{2}}}$$

and finally the length is given by

$$L = \frac{1}{2\,k}\int_{0}^{\alpha}\frac{d\theta}{\sqrt{\sin^2\frac{\alpha}{2} - \sin^2\frac{\theta}{2}}}$$

Now make the following substitutions;

$$\rho = \sin\frac{\alpha}{2}$$

$$\rho\,\sin\phi = \sin\frac{\theta}{2}$$

also note that

$$\phi = \sin^{-1}\left(\frac{\sin\frac{\theta}{2}}{\sin\frac{\alpha}{2}}\right)$$

By taking the differentials, dΘ is found to be;

$$\frac{1}{2}\cos\frac{\theta}{2}d\theta = \rho\,\cos\phi d\phi$$

or

$$d\theta = \frac{2\,\rho\,\cos\phi d\phi}{\sqrt{1-\sin^2\frac{\theta}{2}}} = \frac{2\,\rho\,\cos\phi d\phi}{\sqrt{1-\rho^2\sin^2\phi}}$$

Therefore, by substituting dΘ into the equation for L gives;

$$L = \frac{1}{2\,k}\int_{\sin^{-1}(0)}^{\sin^{-1}(1)} \frac{2\,\rho\,\cos\phi d\phi}{(\sqrt{\rho^2-\rho^2\sin^2\phi})(\sqrt{1-\rho^2\sin^2\phi})}$$

$$= \frac{1}{k}\int_0^{\frac{\pi}{2}} \frac{\cos\phi d\phi}{(\sqrt{1-\sin^2\phi})(\sqrt{1-\rho^2\sin^2\phi})}$$

$$L = \frac{1}{k}\int_0^{\frac{\pi}{2}} \frac{\cos\phi d\phi}{\cos\phi\sqrt{1-\rho^2\sin^2\phi}}$$

$$= \frac{1}{k}\int_0^{\frac{\pi}{2}} \frac{d\phi}{\sqrt{1-\rho^2\sin^2\phi}}$$

Finally;

$$L = \frac{1}{k}K(\rho)$$

In this equation L is a known quantity, but k and ρ are both unknown quantities, thus a second equation is needed. The horizontal distance, x, is known (half the pin-to-pin distance). Note that dx = ds cos Θ, which gives;

$$dx = -\frac{1}{2\,k}\frac{\cos\theta\,d\theta}{\sqrt{\sin^2\frac{\alpha}{2} - \sin^2\frac{\theta}{2}}}$$

$$x = -\frac{1}{2\,k}\int_{\alpha}^{0}\frac{\cos\theta\,d\theta}{\sqrt{\sin^2\frac{\alpha}{2} - \sin^2\frac{\theta}{2}}} = \frac{1}{2\,k}\int_{0}^{\alpha}\frac{\cos\theta\,d\theta}{\sqrt{\sin^2\frac{\alpha}{2} - \sin^2\frac{\theta}{2}}}$$

Using the same substitutions as in the length equation shows;

$$x = \frac{1}{k}\int_{0}^{\frac{\pi}{2}}\frac{\cos\theta\,d\theta}{\sqrt{1 - \rho^2\sin^2\theta}}$$

where

$$\cos\theta = 2\cos^2\frac{\theta}{2} - 1$$

then the equation for x becomes;

$$x = \frac{1}{k}\int_{0}^{\frac{\pi}{2}}\frac{2\cos^2\frac{\theta}{2}\,d\theta}{\sqrt{1 - \rho^2\sin^2\phi}} - \frac{1}{k}\int_{0}^{\frac{\pi}{2}}\frac{1}{\sqrt{1 - \rho^2\sin^2\phi}}$$

Notice that the second integral is the same one used to evaluate L.

$$x = \frac{2}{k}\int_{0}^{\frac{\pi}{2}}\frac{\cos^2\frac{\theta}{2}\,d\phi}{\sqrt{1 - \rho^2\sin^2\phi}} - L$$

Substituting trigonometric identities yields the following equation for x;

$$x = \frac{2}{k}E(\rho) - L$$

Again k and ρ are unknowns, but combining the equations for x and L eliminates k and gives;

$$K(\rho) = \frac{2\,L}{L + x}E(\rho)$$

A computer program was written in BASIC to solve for ρ.

Since

$$\rho = \sin\frac{\alpha}{2}$$

and α is known, k can be calculated using the following equation;

$$k = \frac{K(\rho)}{L}$$

The following equations show how to determine the deflection at any given point along the length of the batten, note that dy=sinΘ ds. First consider the case for the maximum deflection.

$$y_{max} = \frac{1}{k}\int_0^{\frac{\pi}{2}} \frac{\sin\theta d\theta}{\sqrt{1 - \rho^2 \sin^2\phi}}$$

where;

$$\sin\theta = 2 \sin\frac{\theta}{2}\cos\frac{\theta}{2}$$

$$y_{max} = \frac{1}{k}\int_0^{\frac{\pi}{2}} \frac{2(\rho \sin\phi)\sqrt{1 - \rho^2 \sin^2\phi}}{\sqrt{1 - \rho^2 \sin^2\phi}} d\phi = \frac{2\rho}{k}\int_0^{\frac{\pi}{2}} \sin\phi d\phi = \frac{2\rho}{k}$$

Consider the following;

$$\phi = \sin^{-1}\left(\frac{\sin\frac{\theta}{2}}{\sin\frac{\alpha}{2}}\right)$$

If the lower limit of integration is considered at the loaded end and the upper limit is just short of the fixed end of the batten, the Θ takes on values from ß to α, where $0 \le ß \le \alpha$. Then the following happens to ϕ;

$$\phi = \sin^{-1}\left(\frac{\sin\frac{\theta}{2}}{\sin\frac{\alpha}{2}}\right) = \sin^{-1}\left(\frac{\sqrt{\frac{1 - \cos\theta}{2}}}{\sqrt{\frac{1 - \cos\alpha}{2}}}\right)$$

By examining the following equation for ϕ, at the points where $\Theta=\beta$ and $\Theta=\alpha$ the limits of integration are found;

$$\phi = \sin^{-1}\sqrt{\frac{1 - \cos\theta}{1 - \cos\alpha}}$$

$\Theta=\beta$;

$$\phi = \sin^{-1}\sqrt{\frac{1 - \cos\beta}{1 - \cos\alpha}}$$

$\Theta=\alpha$;

$$\phi = \sin^{-1}(1) = \frac{\pi}{2}$$

Thus the resultant incremental deflection is given by;

$$\Delta y = \frac{2\rho}{k} \int_{\sin^{-1}\sqrt{\frac{1 - \cos\beta}{1 - \cos\alpha}}}^{\frac{\pi}{2}} \sin\phi d\phi = \frac{2\rho}{k} \cos\phi \Big|_{\frac{\pi}{2}}^{\sin^{-1}\sqrt{\frac{1 - \cos\beta}{1 - \cos\alpha}}}$$

APPENDIX B

Deflection/Moment Equations for Short Batten Segments:

Symbols:

σ: stress, Pa
M: moment, N-m
c: distance from neutral axis, m
I: area moment of inertia, m^4
x: distance from point 0, m
y: deflection of batten segment, m
L: length of batten segment, m
Θ: angle between tangent to arc and x-coordinate, degree
Z: translation distance of point (o) due to rotation of mounting block, m
C1: constant of integration
C2: constant of integration

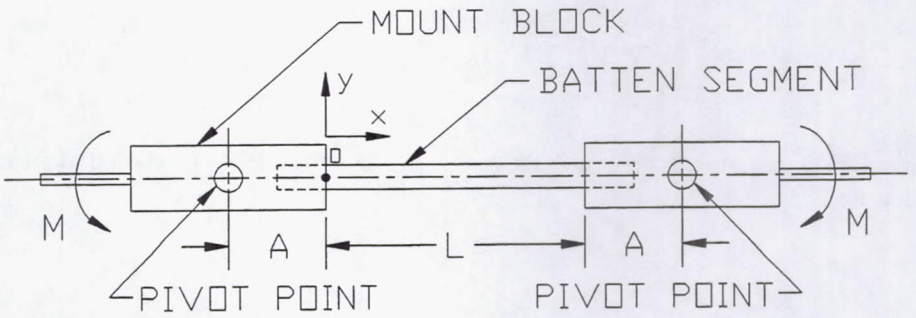

Target Stress: (Based on elastic flexure formula)

$$\sigma = \frac{M\,c}{I}$$

Consider the following formula for small elastic deflections where E*I is the flexural rigidity and M is the bending moment;

$$\frac{d\theta}{dx} = \frac{M}{E\,I}$$

Multiplying both sides by dx and integrating gives;

$$\theta = \frac{M}{E\,I}(x) + C_1$$

Also consider the following elastic deflection formula;

$$\frac{d^2y}{dx^2} = \frac{M}{E\,I}$$

Multiplying both sides by dx^2 and integrating twice gives the following;

$$y = \frac{M}{E\,I}\left(\frac{X^2}{2}\right) + C_1(x) + C_2$$

To determine the constants of integration the examination of the boundary conditions is required.
At x=0, y=0 which results in C_2=0.
At x=½L, Θ=0 which yields;

$$C_1 = -\frac{M}{E\,I}\left(\frac{L}{2}\right)$$

At x=0, $\Theta=C_1$.

$$\theta = -\frac{M}{E\,I}\left(\frac{L}{2}\right)$$

For x=½L, y becomes;

$$y = \frac{M}{E\,I}\left(\frac{L^2}{8}\right) + \left(-\frac{M}{E\,I}\right)\left(\frac{L}{2}\right)\frac{L}{2} = -\frac{M\,L^2}{8\,E\,I}$$

The translation (Z) of the batten at point O in the positive y-direction due to the rotation of the mounting block about its pivot point is;

$$Z = A\sin\theta$$

Therefore, the measured deflection in the positive y-direction, at x=½L, to provide the desired level of stress (σ) is;

$$deflection = Z + y$$

REPORT DOCUMENTATION PAGE

Form Approved
OMB No. 0704-0188

1. AGENCY USE ONLY (*Leave blank*)	2. REPORT DATE	3. REPORT TYPE AND DATES COVERED
	December 1994	Technical Memorandum

4. TITLE AND SUBTITLE

Atomic Oxygen Durability Evaluation of the Flexible Batten for the Photovoltaic Array Mast on Space Station

5. FUNDING NUMBERS

WU-233-01-OE

6. AUTHOR(S)

Curtis R. Stidham, Sharon K. Rutledge, Edward A. Sechkar, David S. Flaherty, David M. Roig, and Jonathan L. Edwards

7. PERFORMING ORGANIZATION NAME(S) AND ADDRESS(ES)

National Aeronautics and Space Administration
Lewis Research Center
Cleveland, Ohio 44135-3191

8. PERFORMING ORGANIZATION REPORT NUMBER

E-9270

9. SPONSORING/MONITORING AGENCY NAME(S) AND ADDRESS(ES)

National Aeronautics and Space Administration
Washington, D.C. 20546-0001

10. SPONSORING/MONITORING AGENCY REPORT NUMBER

NASA TM-106798

11. SUPPLEMENTARY NOTES

Prepared for the 1995 International Solar Energy Conference cosponsored by ASME, JSME, and JSES, Lahaina, Maui, Hawaii, March 19-24, 1995. Curtis R. Stidham, NYMA, Inc., 2001 Aerospace Parkway, Brook Park, Ohio 44142 (work funded by NASA Contract NAS3-27186); Sharon K. Rutledge, NASA Lewis Research Center; Edward A. Sechkar, David S. Flaherty, and David M. Roig, Cleveland State University, Physics Department, Cleveland, Ohio 44115; Jonathan L. Edwards, Ohio Aerospace Institute, 22800 Cedar Point Road, Cleveland, Ohio 44142. Responsible person, Sharon K. Rutledge, organization code 5480, (216) 433-2219.

12a. DISTRIBUTION/AVAILABILITY STATEMENT

Unclassified - Unlimited
Subject Categories 24 and 37

This publication is available from the NASA Center for Aerospace Information, (301) 621-0390.

12b. DISTRIBUTION CODE

13. ABSTRACT ***(Maximum 200 words)***

A test program was conducted at the National Aeronautics and Space Administration's Lewis Research Center (LeRC) to evaluate the long term low Earth orbital (LEO) atomic oxygen (AO) durability of a flexible (fiberglass-epoxy composite) batten. The flexible batten is a component used to provide structural rigidity in the photovoltaic array mast on Space Station. The mast is used to support and articulate the photovoltaic array, therefore, the flexible batten must be preloaded for the 15 year lifetime of an array blanket. Development hardware and composite materials were evaluated in ground testing facilities for AO durability and dynamic retraction-deployment cyclic loading representative of expected full life in-space application. The CV1144 silicone (AO protective) coating was determined to provide adequate protection against AO degradation of the composite material and provided fiber containment, thus the structural integrity of the flexible batten was maintained. Both silicone coated and uncoated flexible battens maintained load carrying capabilities. Results of the testing did indicate that the CV1144 silicone protective coating was oxidized by AO reactions to form a brittle glassy (SiO_2) skin that formed cracking patterns on all sides of the coated samples. The cracking was observed in samples that were mechanically stressed as well as samples in non-stressed conditions. The oxidized silicon was observed to randomly spall in small localized areas, on the flexible battens that underwent retraction-deployment cycling. Some darkening of the silicon, attributed to vacuum ultraviolet (VUV) radiation, was observed.

14. SUBJECT TERMS	15. NUMBER OF PAGES
Atomic oxygen; Fiberglass-epoxy; Composite testing	24
	16. PRICE CODE: A03

17. SECURITY CLASSIFICATION OF REPORT	18. SECURITY CLASSIFICATION OF THIS PAGE	19. SECURITY CLASSIFICATION OF ABSTRACT	20. LIMITATION OF ABSTRACT
Unclassified	Unclassified	Unclassified	